SEVENTEENTH INTERNATIONAL WORKSHOP ON
rare-earth magnets and their applications
August 18-22, 2002, Newark, Delaware

IMPROVING EXCHANGE-SPRING MAGNETS WITH INTERFACIAL MODIFICATION

J. S. JIANG, J. E. PEARSON AND S. D. BADER
Materials Science Division, Argonne National Laboratory, Argonne IL 60439

J. P. LIU
Institute for Micromanufacturing, Louisiana Tech University, Ruston, LA 71272

Using magnetic thin film multilayers as model exchange-spring systems proves to be the promising intellectual path that helps generate the mechanistic and materials insights needed to create high-performance permanent magnet materials. We demonstrate a new route to improve exchange-spring magnets whereby the hard/soft interface in epitaxial Sm-Co/Fe and Sm-Co/Co bilayer thin film structures is modified via thermal processing. The effect of thermal processing is modeled with a graded interfacial region across which the material parameters vary linearly. We discuss the mechanism for improved exchange-spring behavior and the implication on magnet processing toward realizing the full potential of the exchange-spring principle.

1. Introduction

The exchange-spring magnet[1], which is based on interfacial exchange coupled soft and hard ferromagnetic nano-phases, exemplifies the materials-by-design approach at the nanometer scale to create high performance permanent magnet materials. In principle, the hard phase in an exchange-spring magnet supplies magnetic anisotropy to resist magnetization reversal, while the soft phase provides the high magnetization necessary for remanence enhancement and high energy product. It has been predicted that exchange-spring magnets have the potential to outperform Nd-Fe-B, currently the best commercially available permanent magnet material.[2]

Exchange-spring magnets have been fabricated mainly by rapid-quenching and subsequent annealing or mechanical alloying.[3-5] Such bulk processing techniques are necessitated by the large scale of permanent magnet applications.[6] However, exchange-spring magnets have yet to fully deliver on the promise of significantly enhanced properties. Bulk processing yields nanocomposites with randomly dispersed and randomly oriented hard grains. Their maximum energy product $(BH)_{max}$, although improved over single phase isotropic hard magnets, is still significantly lower than that of oriented single-phase magnets. Great efforts have been devoted to optimize the microstructure and to improve the technical properties of bulk-processed exchange-spring magnets.[5,7] Nevertheless, the complexities of random nanocomposite exchange-spring magnets often make it difficult to even identify the factors that affect the magnetization reversal process in the first place.

On the other hand, thin film magnetic heterostructures such as multilayers and superlattices have long proven essential in elucidating a variety of magnetic phenomenon[8]. Thin film deposition techniques provide the advantages of nanometer-scale control of the material parameters in the growth direction. Moreover, epitaxial growth allows the magnetic properties to be tailored by controlling the microstructure, crystal orientation and magnetic anisotropies in the plane of the thin film. Such relatively simple structures are also amenable to a wider variety of microscopic characterization tools and numerical modeling than are complex random nanocomposites. Magnetic heterostructures such as coupled hard/soft bilayers and superlattices have proven to be a successful model system for unveiling the fundamental magnetization processes and the microstructure-properties relationships in exchange-spring magnets.[9,10]

In order to fully exploit the benefit of remanence enhancement in exchange-spring magnets, the soft phase must couple effectively to the hard phase. Shown in Fig. 1. are the hysteresis and *BH* curves of a Sm-Co(200Å)/Fe(100Å) exchange-spring bilayer structure calculated from numerical simulation. The magnetization reversal is characterized by the nucleation of a quasi-Bloch wall in the soft phase at the nucleation field H_N (or the exchange field H_{ex}. In the case of a perfectly soft layer, H_N is the same as H_{ex}) and the irreversible switching of the hard phase at H_{irr}. Although such a composition has a theoretical $(BH)_{max}$ of 34 MGOe, the early reversal of Fe at H_N limits $(BH)_{max}$ to ~21 MGOe. These simulated results agree well with those measured from actual sputtered epitaxial Sm-Co/Fe exchange-spring bilayer structures.[11]

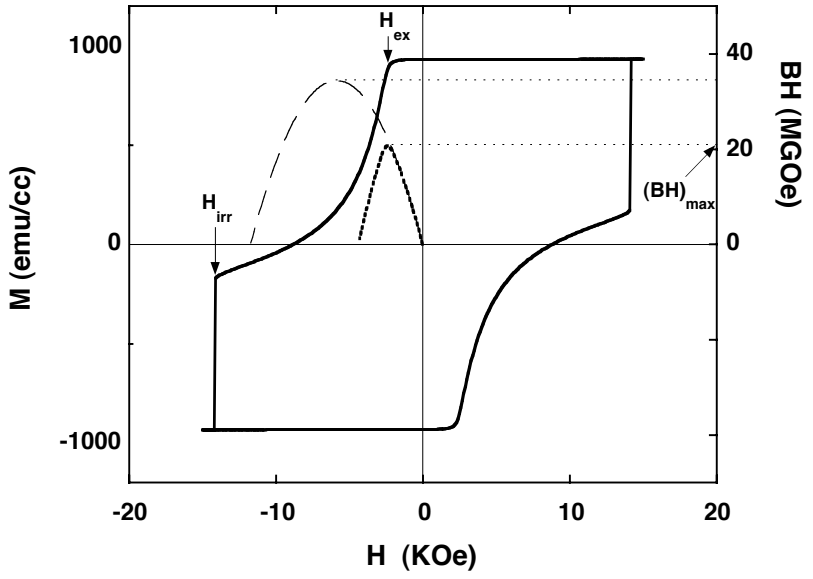

Figure 1. Calculated hysteresis loop (solid) and the BH curve (dotted) of a Sm-Co(200Å)/Fe(100Å) exchange-spring bilayer structure. Also shown is the hypothetical BH curve (dashed) assuming the Fe remains rigidly coupled to Sm-Co.

Two approaches are commonly taken to enhance the effectiveness of exchange coupling between the soft and hard phases. One involves using additives to inhibit grain growth of the soft and hard phases. But the non-magnetic additives reduce the total magnetization and the typical grain size is still on the order of 100 Å. If the size of the hard phase grains becomes too small, they become magnetically unstable against repeated field cycling.[12] Furthermore, this approach demands great metallurgical insight, and remains a trial-and-error process. The other approach centers on improving the interface coherence to increase the exchange coupling between the hard and soft phases. However, it is the incoherent reversal of the soft layer that makes H_{ex} significantly lower than that estimated from the Stoner-Wohlfarth model.[13] The upper limit for H_{ex} in the case of perfect hard/soft interfacial coupling was given by Goto *et al.* [14]:

$$H_{ex} = \pi^2 A_{soft} / 2M_{soft} t_{soft}^2, \quad (1)$$

where A_{soft}, M_{soft}, and t_{soft} are the exchange constant, magnetization and thickness of the soft layer, respectively. For 200 Å of Fe, $H_{ex} \cong 2$ kOe. There is not much headroom to be gained by striving for atomically coherent interfaces.

In this article, we introduce an alternative to conventional magnet processing routes towards realizing the full potential of exchange-spring magnets. We report the effect of thermal processing on the magnetization behavior of epitaxially grown Sm-Co/Fe and Sm-Co/Co exchange-spring bilayer structures. The potential of using interdiffusion for tailoring exchange-spring magnets was recently explored by Crew *et al.*[15], who annealed bilayer CoPt/Co films to induce interdiffusion of the Co and CoPt layer and to create changes in the phase constitution and proportions. They observed a tantalizing change from the two-phase demagnetization behavior in the as-deposited sample to single-phase demagnetization behavior in a high-temperature annealed sample. However, the hard magnetic properties of their annealed sample were actually degraded because it developed a significant perpendicular magnetic anisotropy and the annealing produced an increase in the relative amount of the soft phase with an associated decrease in the hard phase amount. With epitaxial Sm-Co/Fe and Sm-Co/Co exchange-spring bilayers, we aim to create a graded interfacial region where the material parameters vary gradually by promoting intermixing of Sm-Co with Fe or Co, rather than just altering the proportion of the hard and soft phases. The graded interface fundamentally changes the magnetization reversal behavior: the onset of the magnetization reversal happens at larger field, the hysteresis loops become more single-phase-like and the quasi-Bloch wall nucleated during reversal is kept out of the hard phase, leading to fully reversible magnetization and potentially improved magnetic stability.

2. Sample Preparation

We fabricated the Sm-Co/Fe and Sm-Co/Co exchange-spring bilayers by DC magnetron sputtering. The Sm-Co layer with a nominal composition of Sm_2Co_7 was grown epitaxially at 400°C onto a single crystal MgO(110) substrate coated with a 200 Å Cr(211) buffer layer, resulting in an in-plane uniaxial magnetic anisotropy with the easy axis along the MgO[001] direction and a room temperature anisotropy field estimated at

20-25 T.[16] The thickness of the Sm-Co layer in all samples was kept at 200 Å. Following the deposition of the Sm-Co layer, Fe or Co layers were deposited either at 400°C immediately, or at 70-100°C after the Sm-Co layer was cooled. The Fe or Co layers are 100 Å or 200 Å in thickness. We also fabricated Sm-Co/Fe bilayers with the Fe layer deposited at 400°C after the Sm-Co layer had been kept at 400°C for about one hour, the time needed for the substrate holder to cool from 400°C to 100°C. The purpose was to check if the exposed Sm-Co surface became contaminated during the cool down. The samples were finally covered with a 100 Å layer of Ag. Because Ag is mutually insoluble with Fe or Co, interdiffusion is unlikely to occur at the Fe/Ag and Co/Ag interfaces during deposition or when the samples were annealed at high temperatures afterwards. Annealing of the exchange-spring samples was done with the same heater inside the deposition chamber. Pieces were cut from the as-deposited samples and annealed for one hour at temperatures ranging from 200°C to 400°C in a vacuum of 1×10^{-8} Torr. From here on, we denote a sample by T_S (substrate temperature) or T_A (annealing temperature), which is the last temperature the soft layer has been subjected to during its processing.

3. Results and Discussions

The layer structure and the interface characteristics of the samples were examined by analyzing the x-ray reflectivity data collected using Cu K_α radiation. Magnetic hysteresis loop measurements were performed using an Alternating Gradient magnetometer (AGM) with the applied magnetic field along the easy direction of the Sm-Co layer. The reversibility of the exchange-springs was characterized by measuring the DC demagnetization remanence (DCD) curves. For the DCD measurements, the samples were repeatedly saturated in a +1.4 T field before the demagnetizing field was applied.

Shown in Fig. 2 are the room-temperature hysteresis loops for three samples: Sm-Co(200Å)/Fe(200Å, T_S = 70°C), Sm-Co(200Å)/Fe(200Å, T_A = 300°C), and Sm-Co(200Å)/Fe(200Å, T_S = 400°C). The first sample shows a two-stepped hysteresis loop: the Fe layer starts to reverse at a nucleation field H_N ~1 kOe and the Sm-Co layer switches irreversibly at ~7.5 kOe. The low nucleation field indicates that the Fe layer is not effectively coupled to the Sm-Co layer. The switching fields are identical to the ones reported previously[11]. After annealing at 300°C, H_N increases to ~1.2 kOe while the Sm-Co switching field is reduced slightly to ~7.2 kOe. For the Sm-Co(200Å)/Fe(200Å, T_S = 400°C) sample, H_N further increases to 1.6 kOe and the Sm-Co switches at a still lower ~6 kOe. One might be tempted to attribute the low H_N in the Sm-Co(200Å)/Fe(200Å, T_S = 70°C) sample to reduced interface coupling due to possible contamination when the Sm-Co was exposed during cooling. However, the Sm-Co(200Å)/Fe(200Å, T_S = 400°C) sample where the Sm-Co was left exposed at 400°C for one hour showed no discernable difference in magnetization behavior from the one with Fe deposited immediately. Had there been a reduction in interfacial exchange coupling due to contamination during the one-hour delay, the nucleation field would have been much lower, given that the Sm-Co layer was kept at 400°C rather than being cooled. The thermal processing increases the

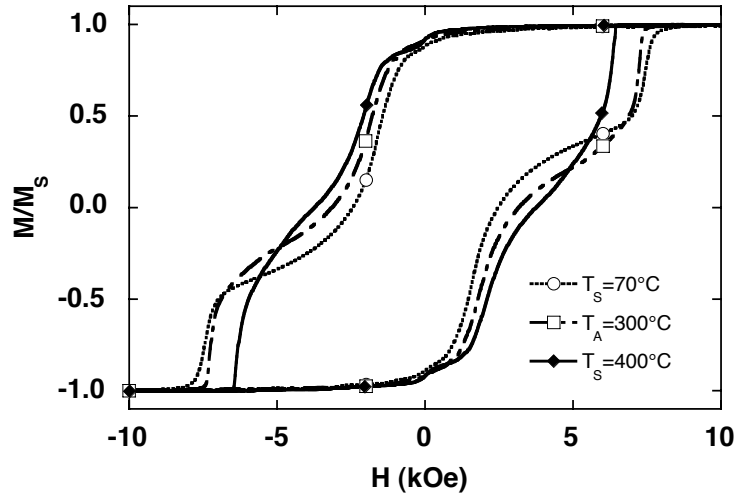

Figure 2. Normalized room-temperature hysteresis loops for three Sm-Co(200 Å)/Fe(200 Å) samples deposited or annealed at various temperatures.

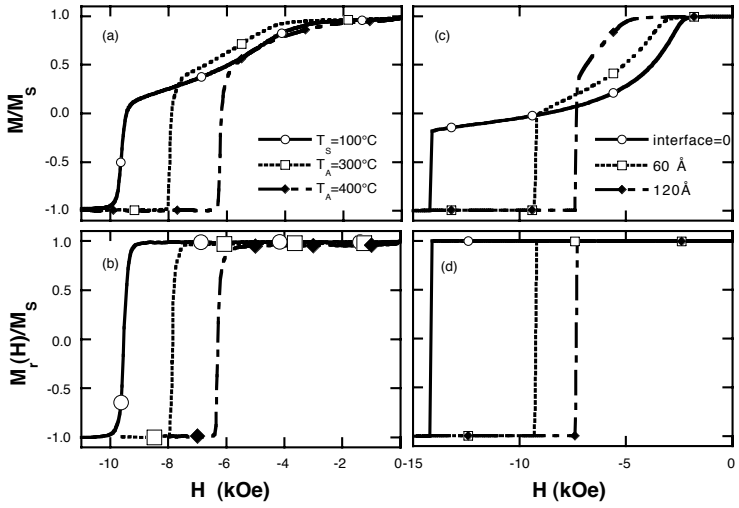

Figure 3. (a) The demagnetization and (b) the dc demagnetization remanence curves for Sm-Co(200 Å)/Fe(100 Å) samples annealed at various temperatures. (c) The demagnetization and (d) the dc demagnetization remanence curves calculated for Sm-Co(200 Å)/Fe(100 Å) bilayers with interfacial regions of various thickness.

$(BH)_{max}$ value from 9.4 MGOe for the T_S = 70°C sample, to 12 MGOe for the T_A = 300°C sample, to 14.1 MGOe for the T_S = 400°C sample.

The change in magnetization behavior is even more pronounced in samples with thinner Fe layers. Shown in Fig. 3(a) are the demagnetization branches of the hysteresis loops for Sm-Co(200Å)/Fe(100Å) samples with T_S = 100°C, T_A = 300°C and 400°C. At T_A=300°C, the onset of the Fe layer reversal increases to over 4 kOe, while the switching field of the hard layer becomes reduced. After annealing at 400°C, the hysteresis becomes single-phase like with a coercive field greater than 6 kOe. The $(BH)_{max}$ value increases from 24 MGOe for the as-deposited sample to 27.7 MGOe for the T_A=300°C sample, and then decreases to 22.4 MGOe for the 400°C sample. There is some rounding at the shoulder which is indicative of some inhomogeneous reversal. The DC demagnetization remanence curves, which measure the remanent magnetization after a reversal field has been applied, are shown in Fig. 3(b). All samples have sharp step-like DC demagnetization remanence curves, indicating a very narrow distribution of the hard layer switching fields and full reversibility of the soft layer magnetization. Particularly noteworthy is the sample with T_A = 400°C. It has a nearly square demagnetization loop, yet the magnetization is fully reversible. In contrast, most nanophase hard magnets show significant irreversible magnetization due to partial reversal of the hard phase, even though their hysteresis loops may appear single-phase-like.[5,15]

The intrinsic properties of the Sm-Co layer could not have been altered by annealing because the annealing temperatures never exceeded the deposition temperature of Sm-Co. And since Ag is mutually insoluble with Fe and Co, the Fe/Ag or Co/Ag interfaces should have remained intact as well. The likely cause for the change in the magnetization behavior of the thermally processed samples is that thermal processing had altered the interface characteristics. The layer thickness and roughness parameters were extracted by fitting the reflectivity data using the WinGIXA software[17], which is based on the Parratt formalism modified to include roughness.[18,19] Figure 4 shows the

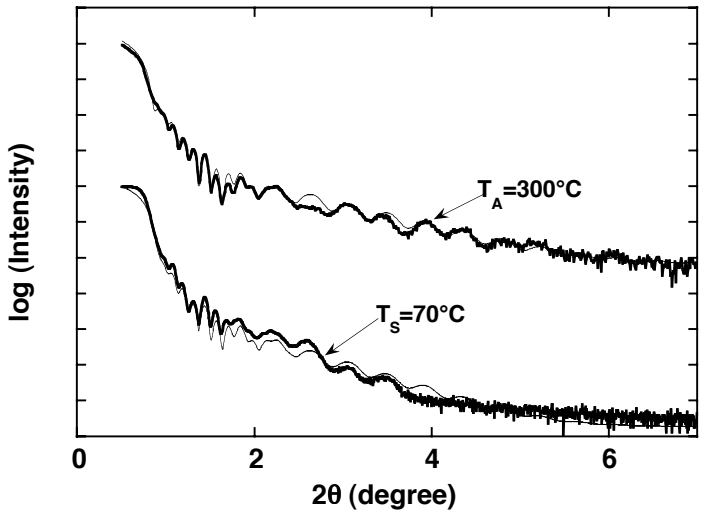

Figure 4. Measured (thick line) and fitted (thin line) x-ray reflectivity curves of as-deposited (T_S=70°C) and annealed (T_A=300°C) Sm-Co/Fe samples. The curves are displaced vertically for clarity.

Table 1: Layer thickness and roughness obtained form fitting X-ray reflectivity data. The numbers are in Å.

Layer	Thickness (roughness) T_S= 70°C	Thickness (roughness) T_A= 300°C
MgO	(5.1)	(4.1)
Cr	200.4 (6.1)	200.4 (4.3)
Sm-Co	195.9 (42.0)	195.9 (33.0)
Fe	181.3 (18.6)	181.3 (18.6)
Ag	143.4 (72.0)	143.4 (86.7)

measured and fitted x-ray reflectivity curves of the Sm-Co(200Å)/Fe(200Å, T_S = 70°C) sample and those after the sample has been annealed at T_A = 300°C. The intensity oscillation in the reflectivity curve of the annealed sample persists at 2θ angles above 6°, whereas that of the as-deposited sample vanishes at 2θ>4°. The disappearance of intensity modulation in reflectivity at high angles is indicative of large roughness from the interior layers of the sample. The thickness and roughness parameters obtained from the fitting are listed in Table 1. The layer thickesses are very close to the nominal values, except for those of the Ag cover layer, which are due possibly to oxidation and handling. The significant difference is in the Sm-Co layer roughness, which is reduced from 42 Å before annealing to 33 Å after annealing. The Sm-Co layer is known to grow in islanding mode initially with large roughness.[16] When the Fe layer is deposited at a low temperature, there is unlikely much intermixing, resulting in a sharp and jagged Sm-Co/Fe interface. In fact, Mössbauer measurement of a similarly prepared sample with a ^{57}Fe probe layer at the interface shows that the Fe hyperfine field increases by a few percent, indicating Co entering only the first couple of monolayers of Fe.[20] Annealing or depositing the Fe layer at elevated temperatures promotes interdiffusion between Sm-Co and Fe, which could have caused the blurring of the interface, leading to the decrease in roughness observed from x-ray reflectivity measurements. This scenario is depicted schematically in Fig. 5(a).

Although the interdiffusion kinetics and the exact nature of the interfacial region are unknown at the present for the thermally processed Sm-Co/Fe bilayers, we can nevertheless establish a model profile of the material parameters and simulate their magnetization behavior. Comparison with experimental observations will determine whether such a model is plausible. It is reasonable to assume that intermixing of Sm-Co and Fe at the interface might create some quasi-binary intermetallic Sm-(Co,Fe) compounds, solid solutions of Sm-Co and Fe, or nanophase mixtures thereof. The interfacial region will transition from Fe-rich at the Fe side to Fe-poor at the Sm-Co side, and its extent depends on the annealing temperature. Such a graded interfacial region will have an associated variation in the intrinsic magnetic properties. Past studies of the $Sm_2(Co_{1-x}Fe_x)_{17}$ alloy phase have found that the incorporation of Fe increases magnetization, the easy-axis symmetry persists up to $x \approx 0.5$, and the Curie temperature varies continuously with x.[21,22] We can therefore assume an interface profile where the

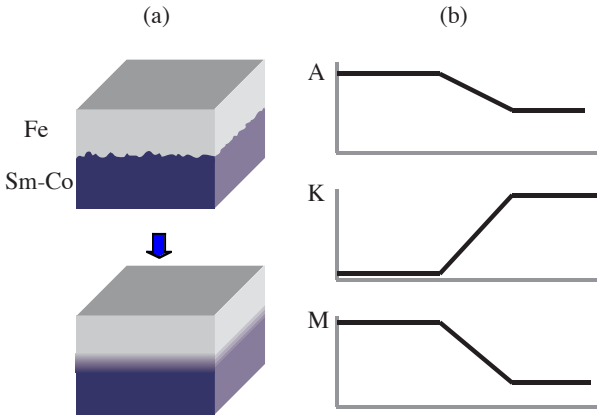

Figure 5. (a) Schematic illustration of the change in interface characteristics of the Sm-Co/Fe bilayer before and after thermal processing. (b) Schematic illustration of the variation in exchange (*A*), anisotropy (*K*) and magnetization (*M*) across a graded Sm-Co/Fe interface.

intrinsic material parameters (such as the exchange constant *A*, the magnetic anisotropy *K*, and the magnetization *M*) ramp linearly, from those of the Fe to those the Sm-Co, as depicted in Fig. 5(b). The width of the interfacial region can be varied to reflect the extent of thermal processing. Based on the profile of material parameters, we simulated the magnetization behavior using the one-dimensional spin chain model previously described.[11] The results for three Sm-Co(200 Å)/Fe(100 Å) exchange-spring bilayers with various widths of the interfacial region are plotted in Figs. 3(c) and 3(d). The simulated loops and demagnetization remanence curves closely resemble those measured experimentally. Whereas the experimental measurements show that the hysteresis loop becomes more single-phase like with increasing annealing temperature, the same trend is seen in the simulated loops with increasing width of the interfacial region. In the part of the modified interfacial region where there used to be soft Fe before annealing, the anisotropy is increased and magnetization decreased. This leads to an increase of the nucleation field. Likewise, the reduced anisotropy and improved effectiveness of soft layer coupling combine to reduce the switching field of the hard layer. The simulated recoil curves (not shown) always completely overlap the demagnetizing curves, leading to fully reversible magnetization.

The numerical simulations also reveal an additional advantage of interface modification where the anisotropy is only gradually increased in part of the interfacial region. In Sm-Co/Co bilayers, it has been shown that the reversal of the Co layer is hysteretic because of the finite anisotropy in the Co layer. Fig. 6 shows the simulated spin profile of a Sm-Co(200 Å)/Fe(100 Å) sample with a 120 Å thick interface at various applied reversal fields. It is worth nothing that the somewhat hardened soft layer never completely reverses, and the spiral spin structure of the quasi-Bloch wall is always confined in the interfacial region, leaving the hard layer undisturbed. This result suggests at improved magnetic stability in interface modified exchange-spring magnets.

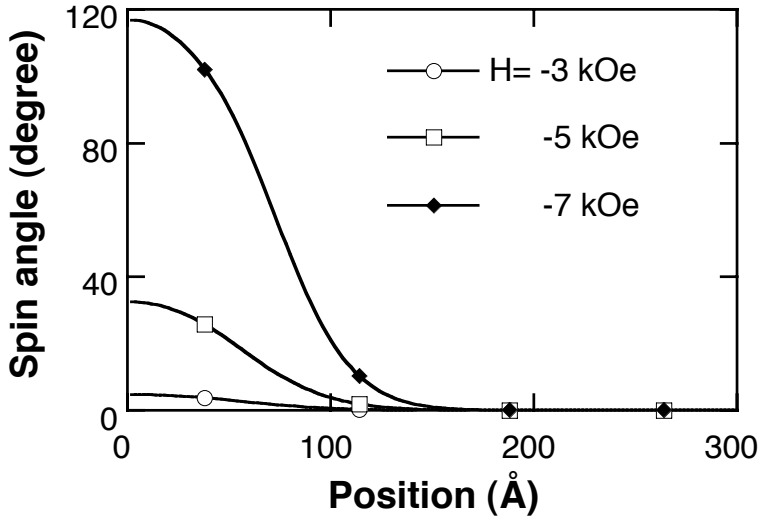

Figure 6. Calculated spin profile of a Sm-Co(200 Å)/Fe(100 Å) bilayer with a 120-Å interfacial region at various reversal fields.

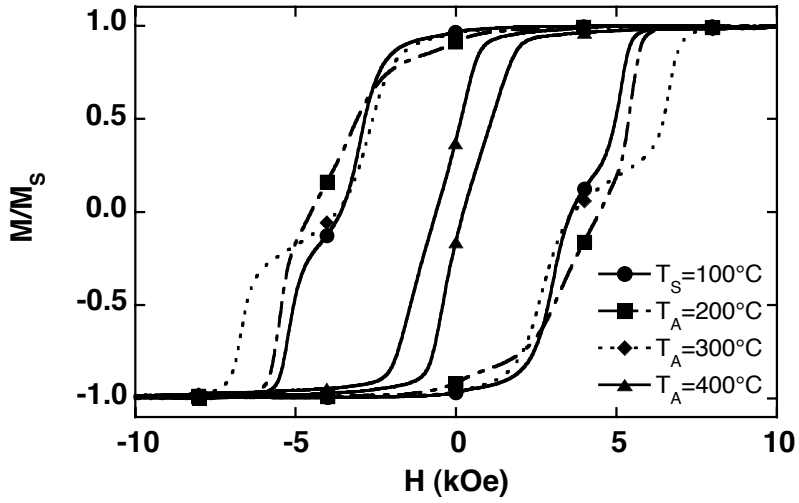

Figure 7. Normalized room-temperature hysteresis loops of as-deposited and annealed Sm-Co(200 Å)/Co(200 Å) samples.

It should be noted that assuming a linear variation in materials parameters across an intermixed interfacial region may not be generally applicable. Indeed, annealing Sm-Co/Co shows no systematic variation of the loop shape on the annealing temperature (Fig. 7), possibly due to the formation of various metastable Sm-Co phases with different

compositions and magnetic properties.[22,23] This result also underscores the limitations of interface modification via thermal processing which, even without the practical uncertainties in controlling the annealing time and temperature, is governed by the thermodynamic principles of phase formation and the actual kinetics of interdiffusion. An athermal means capable of modifying the interface in a more controlled fashion, such as ion beam mixing, is worthy of exploration. Regardless, the remedial nature of interfacial modification means that it can be carried out post-processing, thereby circumventing the difficulty in grain size control encountered by conventional magnet processing routes.

4. Summary

We have demonstrated alternative strategy that overcomes the difficulties of conventional magnet processing techniques to optimize the magnetization behavior of exchange-spring magnets . Annealing or depositing the soft phase at high temperatures induces intermixing at the hard/soft interface, possibly creating a graded interfacial region where the material parameters vary continuously. The graded interface increases the nucleation field and thus improves the energy product. It also keeps the hard phase undisturbed during reversal, leading to potentially improved magnetic stability.

5. Acknowledgements

Work was supported by US DOE BES-MS under Contract No. W-31-109-ENG-38. J. P. Liu acknowledges support by US DOD/DARPA under grant DAAD 19-01-1-0546.

References:

1 E. F. Kneller, R. Hawig, *IEEE Trans. Mag.* **27**, 3588 (1991).
2 R.Skomski, *J. Appl. Phys.* **76**, 7059 (1994).
3 R. Coehoorn, D. B. de Mooij, C. De Waard, *J. Magn. Magn. Mater.* **80**, 101 (1989).
4 J. Ding, P. G. McCormick, and R. Street, *J. Magn. Magn. Mater.* **124**, L1, (1993).
5 For a recent review, see G. C. Hadjipanayis, *J. Magn. Magn. Mater.* **200**, 373(1999).
6 J. M. D. Coey, *Solid State Communications*, 1997, **102**, 101.
7 D. J. Branagan, M. J. Kramer, Y. L. Tang, R. W. McCallum, *J. Appl. Phys.* 85, 5923 (1999).
8 See *e.g. Ultrathin Magnetic Structures*, edited by B. Heinrich and J. A. C. Bland, (Springer, Heidelberg, 1994).
9 E. E. Fullerton, J. S. Jiang, S. D. Bader, *J. Magn. Magn. Mater.* **200**, 392 (1999).
10 J. S. Jiang, S. D. Bader, *Mater. Sci. Technol.* **17**, 1491 (2001).
11 E. E. Fullerton, J. S. Jiang, M. Grimsditch, C. H. Sowers, S. D. Bader, *Phys. Rev.* **B 58**, 12193 (1998).

[12] A. Inomata, J. S. Jiang, C. Y. You, J. E. Pearson, S. D. Bader, *J. Vac. Sci. Technol.* **A18**, 1269 (2000).
[13] T. Nagahama, K. Mibu, T. Shijo, *J. Phys.* **D 31**, 43 (1998).
[14] E. Goto, N. Hayashi, T. Miyashita, K. Nakagawa, *J. Appl. Phys.* **36**, 2951 (1965).
[15] D. C. Crew, J. Kim, L. H. Lewis, K. Barmak, *J. Magn. Magn. Mater.* **233**, 257, (2001)
[16] E. E. Fullerton, J. S. Jiang, Christine Rehm, C. H. Sowers, S. D. Bader, J. B. Patel, and X. Z. Wu, *Appl. Phys. Lett.* **71**, 1579 (1997).
[17] A. J. G. Leenaers, D. K. G. de Boer, *WinGIXA manual*, Philips Analytical X-Ray B. V., Almelo, The Netherlands.
[18] L. G. Parratt, *Phys. Rev.* **95**, 359 (1954).
[19] L. Névot, P. Croce, *Rev. Phys. Appl.* **15**, 761 (1980).
[20] W. Keune, V.E. Kuncser, M. Doi, M. Askin, H. Spies, B. Sahoo, E. Duman, M. Acet, J. S. Jiang, A. Inomata, S. D. Bader, unpublished.
[21] A. E. Ray, K. J. Strnat, *IEEE Trans. Magn.* **MAG-8**, 516 (1972).
[22] K. J. Strnat, R. M. W. Strnat, *J. Magn. Magn. Mater.* **100**, 38 (1991).
[23] J. J. M. Franse, R. J. Radwanski, in *Handbook of Magnetic Materials*, edited by K. H. J. Buschow, vol. 7 (North-Holland, Amsterdam, 1993).